






ORIGINAL RESEARCH

Assessment on gas-polyethylene terephthalate solid interface partial discharge properties of C₄F₇N/CO₂ gas mixture for eco-friendly gas insulating transformer

Song Xiao¹  | Yifan Wang¹  | Chenhua Ren² | Haoran Xia¹  | Yue Zhao³ | Jingzi Qin⁴ | Xiaoxing Zhang⁴  | Yi Luo² | Yi Li¹ 

¹State Key Laboratory of Power Grid Environmental Protection, School of Electrical Engineering and Automation, Wuhan University, Wuhan, Hubei, China

²Beijing International S&T Cooperation Base for Plasma Science and Energy Conversion, Institute of Electrical Engineering, Chinese Academy of Sciences, Beijing, China

³State Grid Anhui Electric Power Company Anhui Electric Power Research Institute, Hefei, Anhui, China

⁴Hubei Engineering Research Center for Safety Monitoring of New Energy and Power Grid Equipment, School of Electrical and Electronic Engineering, Hubei University of Technology, Wuhan, Hubei, China

Correspondence

Yi Li, State Key Laboratory of Power Grid Environmental Protection, School of Electrical Engineering and Automation, Wuhan University, Wuhan, Hubei 430072, China.
Email: li_yi@whu.edu.cn

Yi Luo, Beijing International S&T Cooperation Base for Plasma Science and Energy Conversion, Institute of Electrical Engineering, Chinese Academy of Sciences, Beijing 100190, China.
Email: luoyi@mail.iee.ac.cn

Associate Editor: Dong Dai

Funding information

National Natural Science Foundation of China, Grant/Award Number: 51977159; China Postdoctoral Science Foundation, Grant/Award Number: 2022M712446

Abstract

The eco-friendly insulating gas perfluoroisobutyronitrile (C₄F₇N) is potentially used in gas-insulated transformers (GIT) to replace sulphur hexafluoride (SF₆). However, evaluation of the long-term insulation reliability and gas–solid interface discharge decomposition characteristics of the gas–solid film insulation structure in GIT is indispensable. The authors simulated the gas–solid film insulation structure in GIT and explored the interface partial discharge (PD) characteristics of C₄F₇N/CO₂ gas mixture with polyethylene terephthalate (PET). The effect of gas pressure, mixing ratio on gas–solid interface gas decomposition, PET degradation was investigated, and the interaction mechanism was analysed. It is found that the interface PD generated three degradation regions on a PET film. The gas–solid interface reaction in the electrode contact region and the discharge development trace was significantly higher than that of halation region. The content of gas decomposition products decreases with the increase of gas pressure and the PD intensity of SF₆-PET is inferior to that of C₄F₇N/CO₂ under the same condition. Relevant results provide reference for the development and application of C₄F₇N/CO₂ based GIT.

1 | INTRODUCTION

Transformer is the core equipment in power transmission and distribution systems, and mineral oil is often used as its insulation and cooling medium [1]. However, mineral oil has the disadvantages of low ignition point and non-degradability, and its application in confined spaces, such as buildings and rail transit, bring certain safety hazards [2]. The gas-insulated transformer (GIT) has the advantages of compact structure, low noise and non-flammability, which can meet the needs of special working

conditions [3, 4]. However, the sulphur hexafluoride (SF₆) currently used in GIT is a highly potent greenhouse gas with a global warming potential (GWP) of 24,300 and an atmospheric lifetime of 3200 years [5–7]. The power industry accounts for more than 80% SF₆ usage [8]. With the proposition of the 'net zero' emission target, several countries in the world have gradually introduced SF₆ control or even ban measures [9, 10]. Therefore, the development of eco-friendly insulating gas and equipment is of great significance to achieve the low carbonisation in power industry [11].

Song Xiao, Yifan Wang and Chenhua Ren contributed equally to this work.

This is an open access article under the terms of the [Creative Commons Attribution-NonCommercial](https://creativecommons.org/licenses/by-nc/4.0/) License, which permits use, distribution and reproduction in any medium, provided the original work is properly cited and is not used for commercial purposes.

© 2024 The Authors. *High Voltage* published by John Wiley & Sons Ltd on behalf of The Institution of Engineering and Technology and China Electric Power Research Institute.

In recent years, perfluoroisobutyronitrile (C_4F_7N) has been considered as one of the most promising alternative gases. Its GWP is 2090 and its dielectric strength is more than twice than that of SF_6 [12–14]. Due to the high liquefaction temperature ($-4.7^\circ C$), C_4F_7N needs to be mixed with buffer gases such as CO_2 to meet the minimum operating temperature requirements of the equipment [15, 16]. Scholars have carried out systematic research on the basic insulation, stability and decomposition, material compatibility, biosafety etc. of C_4F_7N/CO_2 gas mixture, and confirmed its application potential in medium and high voltage gas-insulated transmission and distribution equipment [17–19].

The gas–solid insulation structure in GIT is composed of insulating gas and a polyethylene terephthalate (PET) film, which inevitably forms the non-uniform electrical field that is prone to cause partial discharge (PD) even surface flashover [20]. The long-term insulation reliability of gas–solid insulation structure is closely related to the reliability of equipment [21–23].

For example, Okabe et al. studied the discharge characteristics of SF_6 -PET films and found that PD caused the PET film degradation by losing transparency and turning white (called ‘clouding’) and ‘blackening’. Further tests found that the insulation tolerance strength of the ‘clouding’ part did not deteriorate significantly, while the ‘blackening’ part decreased sharply [24]. Ohno et al. pointed out that PD can also induce the decomposition of SF_6 to produce SO_2 , SOF_2 , CF_4 and other decomposition products [25]. Therefore, it is necessary to evaluate the PD and its decomposition characteristics of the gas–solid film in GIT. However, studies on PD and decomposition characteristics of C_4F_7N/CO_2 gas mixture mainly focus on gas phase conditions currently [26–28]. It is found that the decomposition of gas mainly produces fluorocarbons (CF_4 , C_2F_6 , C_3F_8 , C_3F_6 etc.), fluorinated nitriles (CF_3CN , C_2N_2 etc.) and carbon-oxygen compounds (CO , COF_2 etc.) decomposition products. As for the evaluation of gas–solid interface PD characteristics, epoxy resin is mostly utilised [29, 30]. There are few reports on the insulation and decomposition characteristics of C_4F_7N -PET gas–solid interface, which is expected to be explored to evaluate the gas–solid insulation performance in GIT under the fault condition.

In this paper, we simulate the gas-film insulation structure in GIT and test the interface PD characteristics of the C_4F_7N/CO_2 -PET system. The effect of gas pressure, mixing ratio on the decomposition properties are explored and compared with SF_6 . The phase resolved partial discharge (PRPD) pattern and the test results under different conditions contribute to the guidance of fault monitoring and the selection of application conditions of gas mixture. Furthermore, the effect of PD on the morphology and elemental composition of PET and the decomposition mechanism of gas–solid interface are analysed. All the relevant results not only clarify the decomposition characteristics of C_4F_7N/CO_2 -PET gas–solid insulation system but also provide an important reference for the development and application of C_4F_7N/CO_2 -based GIT.

2 | METHODS

2.1 | Test platform

Figure 1a shows the structure of the power frequency discharge test platform, which is mainly composed of the AC voltage regulator (0–380 V), power frequency transformer (100 kV, 50 kVA), protection resistance (10 k Ω), a voltage dividing capacitor (1:1000), a coupling capacitor (500 pF) and test chamber (30 L, 0–0.6 MPa). The coupling capacitor is used to provide a low-resistance, high-frequency channel for the PD pulse current, and the dividing capacitor is used to measure the actual voltage applied to the sample. The pulse current method recommended by IEC60270 is used. The high frequency pulse signal generated by the PD of the sample is measured by the coupling capacitance and the detection impedance, and the relevant data is recorded by the high-speed digital storage oscilloscope (Tektronix DPO5104B, analogue bandwidth is 1 GHz). Two channels of the oscilloscope are utilised to collect the PD signals as well as sinusoidal voltage synchronously.

The gas–solid interface PD test adopts the ‘triple-junction’ model to simulate the interface discharge of C_4F_7N/CO_2 gas mixture and the PET film, that is, PD is triggered by the ‘triple junction point’ at the junction of high voltage electrode, PET film and insulating gas in the model. The size parameters and electric field distribution of the ‘triple junction’ model (based on COMSOL Multiphysics simulation calculation) are shown in Figure 1b,c, respectively. The curvature radius of the rod electrode tip is 10 mm, and the hemisphere tip is polished into a circle with a diameter of 4 mm. The diameter of the plate electrode is 50 mm and the height is 10 mm. The insulating material, that is, the PET film is placed in the middle of the rod–plate electrode and superimposed to a thickness of 3 mm.

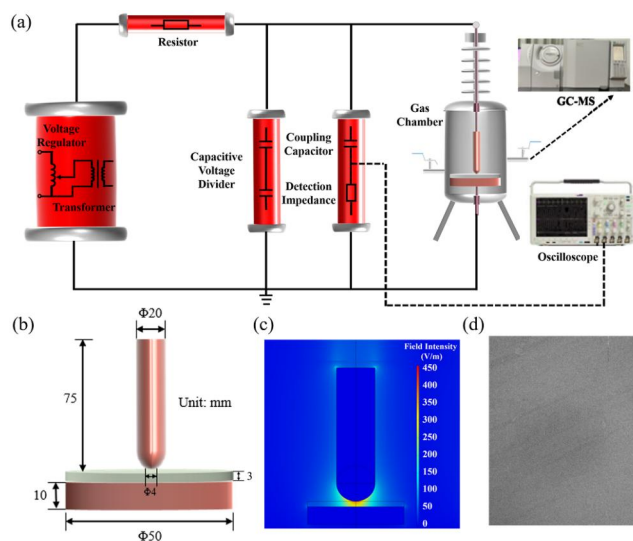


FIGURE 1 The schematic diagram of C_4F_7N/CO_2 gas mixture and the PET film interface partial discharge test platform. (a) Composition and wiring diagram of the test platform, (b) dimension of the electrode model, (c) the electric field distribution of the electrode model, (d) the surface morphology of the PET film before the test.

Figure 1d gives the Scanning Electron Microscope (SEM) morphology of the PET film before the test.

2.2 | Test method

The working pressure of the existing 66–110 kV GIT is mostly 0.23–0.24 MPa (absolute pressure) [31]. Therefore, we set up three groups of gas pressure conditions of 0.2 MPa, 0.24 MPa and 0.3 MPa. According to the liquefaction temperature characteristics of C_4F_7N/CO_2 gas mixture [32], the maximum content of C_4F_7N in the gas mixture under 0.2 MPa, 0.24 MPa, and 0.3 MPa is 18%, 15% and 12%, respectively, when GIT works at $-25^\circ C$. Therefore, we carried out interface PD characteristics tests on 18% $C_4F_7N/82\%CO_2$ (0.2 MPa), 15% $C_4F_7N/85\%CO_2$ (0.24 MPa) and 12% $C_4F_7N/88\%CO_2$ (0.3 MPa).

Before the test, the gas chamber, electrode and PET film were cleaned. Then we eliminated the impurities in the gas chamber and filled the C_4F_7N/CO_2 gas mixture according to the conditions. The PD test was conducted by step-up method (0.5 kV/min). The test voltage was set to 18.5 kV to generate stable PD based on our preliminary exploration, and the test period was set to 72 h. Besides, the 100 AC cycle signals in each measurement were recorded for PRPD analysis (a total record of 2 s). Gas chromatograph-mass spectrometer (GC-MS) was used to analyse the discharge decomposition products of gas mixture every 12 h. At the end of the test, SEM-energy dispersive spectroscopy (energy dispersive spectroscopy) was used to characterise the microstructure, element composition and distribution characteristics of PET films.

2.3 | Theoretical methods

At present, density functional theory (DFT) calculation have been widely utilised to explore the reaction paths and reaction mechanisms of various chemical systems, so as to the gas insulating medium or gas–solid interface interaction [33–36]. Herein, we analysed the reaction mechanism of the C_4F_7N gas–PET solid film based on DFT in this paper. We firstly obtained the most stable structure of each gas and solid molecule by geometric optimisation and then we calculated the energy required for the interaction process. All calculations are based on the DMol³ package of Materials Studio [37, 38]. For geometric optimisation, the generalised approximation method treated by the Perdew–Burke–Ernzerhof (GGA-PBE) functions was used to handle the exchange correlation energy [39]. The convergence criteria of 1.0×10^{-5} Ha, 0.005 Å, and 0.002 Ha/Å for energy tolerance, displacement and maximum force was set, respectively.

Besides, we explored the discharge process of the gas–film interface from the perspective of numerical simulation. Due to the lack of core data such as the collision cross section of C_4F_7N and its main decomposition by-products, we used 80% $N_2/20\%O_2$ as the gas medium to illustrate the interface

discharge development process. The 2D parallel streamer solver with KinEtics (PASSKEy) model was built [40]. The model is based on solving the conservation of mass, momentum and energy equations of different plasma species. The mass conservation equation is given as follows:

$$\frac{\partial n_i}{\partial t} + \nabla \cdot \Gamma_i = S_i \quad (1)$$

$$\Gamma_i = \mu_i n_i E - D_i \nabla n_i \quad (2)$$

Where, n_i stands for the density of electron, ion, radical or neutral species. Γ_i is its flux, and S_i is the source term, which is the sum of the production and loss terms for the species. E is the electric field intensity, μ_i is the mobility and D_i is the diffusion coefficient, respectively.

The deposited charges on dielectric surface was solved by Poisson's equation:

$$\nabla(\epsilon E) = - \sum_{i=1}^{N_{\text{charge}}} q_i n_i - \sigma_s \quad (3)$$

$$\frac{\partial \sigma_s}{\partial t} = \sum_{j=1}^n q_j (-\nabla \cdot \Gamma_j + S_j) \quad (4)$$

$$E = -\nabla \varphi \quad (5)$$

Where, φ is the applied voltage, σ_s is the space charge, ϵ is the dielectric constant, q_j is the charge of species j and N_{charge} is the number of the deposited charges.

The electron energy distribution function was assumed as Maxwellian. The effect of photoionisation was considered and was solved by the three terms Helmholtz equations. The swarm coefficients and reactions rate of electrons were taken from BOLSIG + [41]. The plasma kinetics scheme for N_2/O_2 included 15 species and 34 reactions in total. The pressure of gas mixture was set to 0.1 MPa and the temperature was 300 K. In order to ensure the rationality of the simulation results, the setting of the electrode structure parameters in the simulation was completely consistent with the test conditions. The voltage was also set to 18.5 kV, the rise time was 0.1 ns and the end time was 20.0 ns.

2.4 | Data process

Due to the different pressures of the three different test conditions, the increase of the gas pressure will change the molar concentration of the gas in the chamber when its volume is constant. Since the volume fraction of each decomposition product obtained by the GC-MS cannot directly reflect the change of the actual amount in the chamber, the volume fraction needs to be converted into molar concentration. The chamber in the test is a closed system, so its initial state satisfies the gaseous state equation:

$$PV = nRT \quad (6)$$

In the formula, P and V is the pressure (unit: Pa) and volume (unit: L) of the gas chamber, respectively. n is the amount of substance (unit: mol). T is the thermodynamic temperature (unit: K). R is the molar gas constant, which is a constant value of 8.31×10^3 and the unit is $\text{Pa L K}^{-1} \text{ mol}^{-1}$. The temperature of the initial state of the gas chamber is room temperature $T_0 = 298.15 \text{ K}$, and the three groups of test pressures are 0.2 MPa, 0.24 MPa and 0.3 MPa, respectively. n_0 is the amount of substance of the gas mixture. The molar concentration of the gas mixture in the initial state can be calculated from formula (7):

$$c_0(\text{gas mixture}) = \frac{n_0}{V} = \frac{P}{RT_0} \quad (7)$$

The initial molar concentration of $\text{C}_4\text{F}_7\text{N}/\text{CO}_2$ gas mixture at different pressures is calculated, and the results are shown in Table 1. Since the amount of gas involved in the PD induced decomposition is relatively small (content of the highest decomposition product does not exceed 0.004%), the main components in the gas chamber after the test are still $\text{C}_4\text{F}_7\text{N}$ and CO_2 . Thus, the volume fraction of the decomposition product obtained by GC-MS reflects its proportion of the amount of substance in the gas mixture.

The decomposition products in this test are all from the decomposition of $\text{C}_4\text{F}_7\text{N}$. The initial molar concentration of $\text{C}_4\text{F}_7\text{N}$ in the three groups of tests is 0.001,458 mol/L according to the calculation results using formula (8). Where α is the mixing ratio of $\text{C}_4\text{F}_7\text{N}$:

$$c_0(\text{C}_4\text{F}_7\text{N}) = c_0(\text{gas mixture}) \times \alpha \quad (8)$$

The initial molar concentration of $\text{C}_4\text{F}_7\text{N}$ is the same under the three groups of test conditions. Therefore, the influence of different test conditions on the decomposition of $\text{C}_4\text{F}_7\text{N}$ can be explored by comparing the molar concentration of decomposition products. Herein, φ is set as the volume fraction of the measured decomposition product, and $\varphi_1 = \frac{\varphi}{\alpha}$ belongs to the volume fraction of the decomposition product in $\text{C}_4\text{F}_7\text{N}$. The molar concentration of the decomposition product is calculated as follows:

$$\begin{aligned} c(\text{gas product}) &= c_0(\text{C}_4\text{F}_7\text{N}) \times \varphi_1 = c_0(\text{gas mixture}) \times \alpha \times \frac{\varphi}{\alpha} \\ &= c_0(\text{gas mixture}) \times \varphi \end{aligned} \quad (9)$$

3 | RESULTS AND DISCUSSION

3.1 | Interface PD decomposition characteristics of $\text{C}_4\text{F}_7\text{N}/\text{CO}_2$ -PET

Figure 2 shows the interface PD decomposition characteristics of $\text{C}_4\text{F}_7\text{N}/\text{CO}_2$ with the PET film. The gaseous by-products are the average value calculated by repeating three tests under the same conditions. The main PD decomposition products contain perfluorocarbon gases (CF_4 , C_2F_6 and C_3F_8) and C_2N_2 . For C_2N_2 , due to the lack of standard gas, we use the peak area integral method to represent its relative concentration change. Specifically, the content of CF_4 , C_2F_6 , C_3F_8 and C_2N_2 increased linearly at 0.2–0.3 MPa during 72 h PD, indicating that $\text{C}_4\text{F}_7\text{N}$ continued to decompose. The content of CF_4 was the highest, and the yields of C_2F_6 and C_3F_8 were similar. The variation trend of C_2N_2 peak area is similar to that of C_2F_6 and C_3F_8 .

The molar concentration of decomposition product and the PRPD pattern under different test conditions were shown in Figure 3. It can be found that the molar concentration of CF_4 , C_2F_6 and C_3F_8 is the highest at 0.2 MPa, and the value at 0.24 and 0.3 MPa is similar (Figure 3a,b). The peak area of C_2N_2 demonstrates similar trend with that of C_2F_6 and C_3F_8 . As the initial molar concentration of $\text{C}_4\text{F}_7\text{N}$ is the same under different gas pressure conditions, the higher content of decomposition products at low pressure than that of high pressure indicates that the increase of gas pressure can inhibit the PD decomposition process. This is also consistent with the previous research conclusions on gas phase decomposition characteristics of $\text{C}_4\text{F}_7\text{N}/\text{CO}_2$. In fact, according to the PD statistical characteristics given in Figure 3e–g, the number of PD decreases with gas pressure. Specifically, the magnitude of average discharge per single pulse at 0.2 MPa, 0.24 MPa and 0.3 MPa are 256.85, 250.05 and 248.59 pC, respectively, and the PD number are 1824, 684 and 542, respectively. Although the magnitude of average discharge under different pressures is not much different, the number of PD decreases significantly with the increase of pressure. Relevant PD statistical characteristics confirm that the interface discharge of $\text{C}_4\text{F}_7\text{N}/\text{CO}_2$ -PET is more intense at low pressure, resulting in generating more gas decomposition products.

3.2 | Effect of gas–solid interface discharge on PET morphology and element distribution

Figure 4 shows the morphology of the PET film after the test, and it can be seen that three deterioration regions were generated after 72 h interface discharge. Among them, Region

TABLE 1 The initial concentration of $\text{C}_4\text{F}_7\text{N}/\text{CO}_2$ gas mixture under different pressures.

Gas pressure (MPa)	Molar concentration (mol/L)
0.2	0.0807
0.24	0.0969
0.3	0.1211

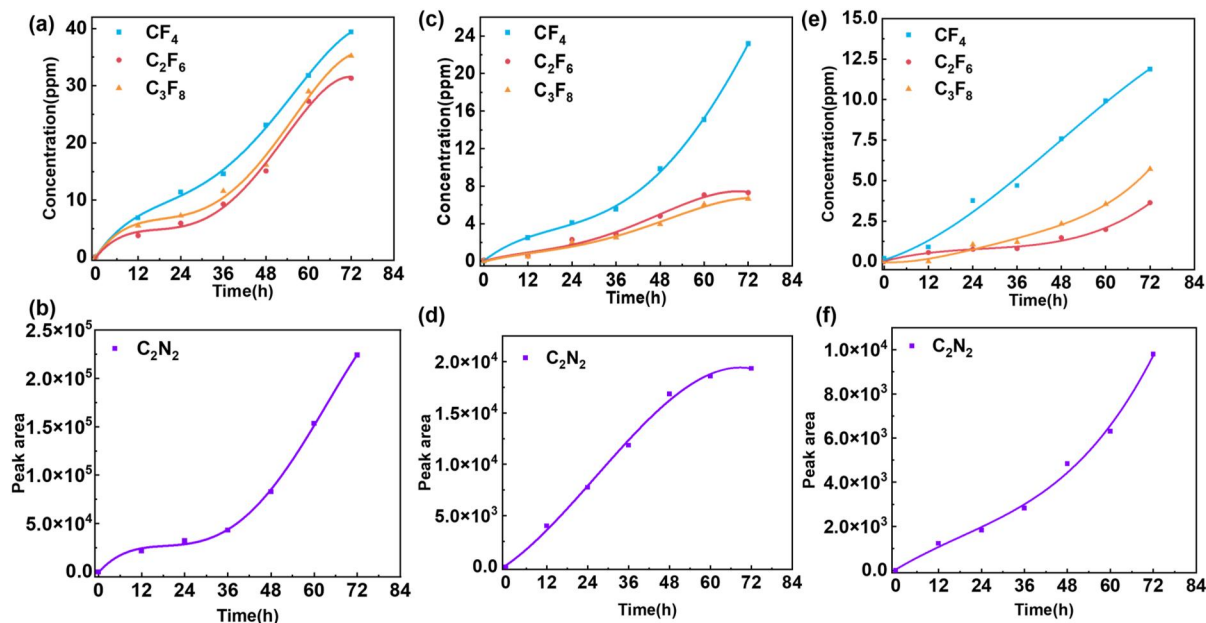


FIGURE 2 Interface discharge induced gaseous decomposition by-products of C_4F_7N/CO_2 -PET film. (a) and (b) 0.2 MPa. (c) and (d) 0.24 MPa. (e) and (f) 0.3 MPa.

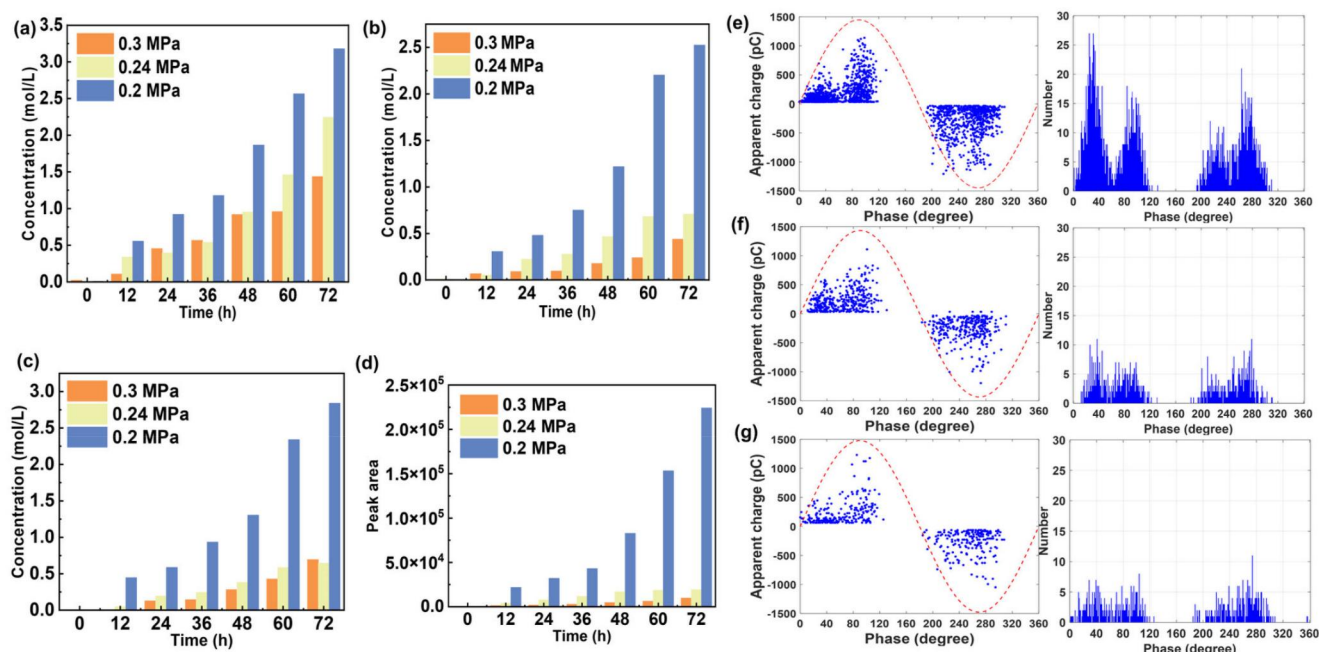


FIGURE 3 Comparison of gas decomposition product concentration and partial discharge statistical characteristics under different test conditions. (a) Concentration of CF_4 . (b) Concentration of C_2F_6 . (c) Concentration of C_3F_8 . (d) Concentration of C_2N_2 . (e) 0.2 MPa. (f) 0.24 MPa. (g) 0.3 MPa.

I is the direct contact part between the electrode and the PET film, and the PET film produces a flaky convex structure caused by ablation after discharge. Region II is located in the halo formed outside Region I and the microscopic morphology is similar to that of Region I. Region III belongs to the outward development trace of interface discharge, and dispersed particles appear on the surface of PET. With the increase of gas pressure, the deterioration of the PET film was

significantly weakened, that is, the interface discharge intensity of C_4F_7N/CO_2 and PET was weak at high gas pressure. In addition, there is no obvious discharge outward development trace at 0.3 MPa (Figure 4c).

Furthermore, Figure 5 shows the elemental composition and content of the three deterioration regions at 0.24 MPa. Except for C, H and O, Cu, F and N elements appeared in Region I after the test, where Cu came from the electrode, and

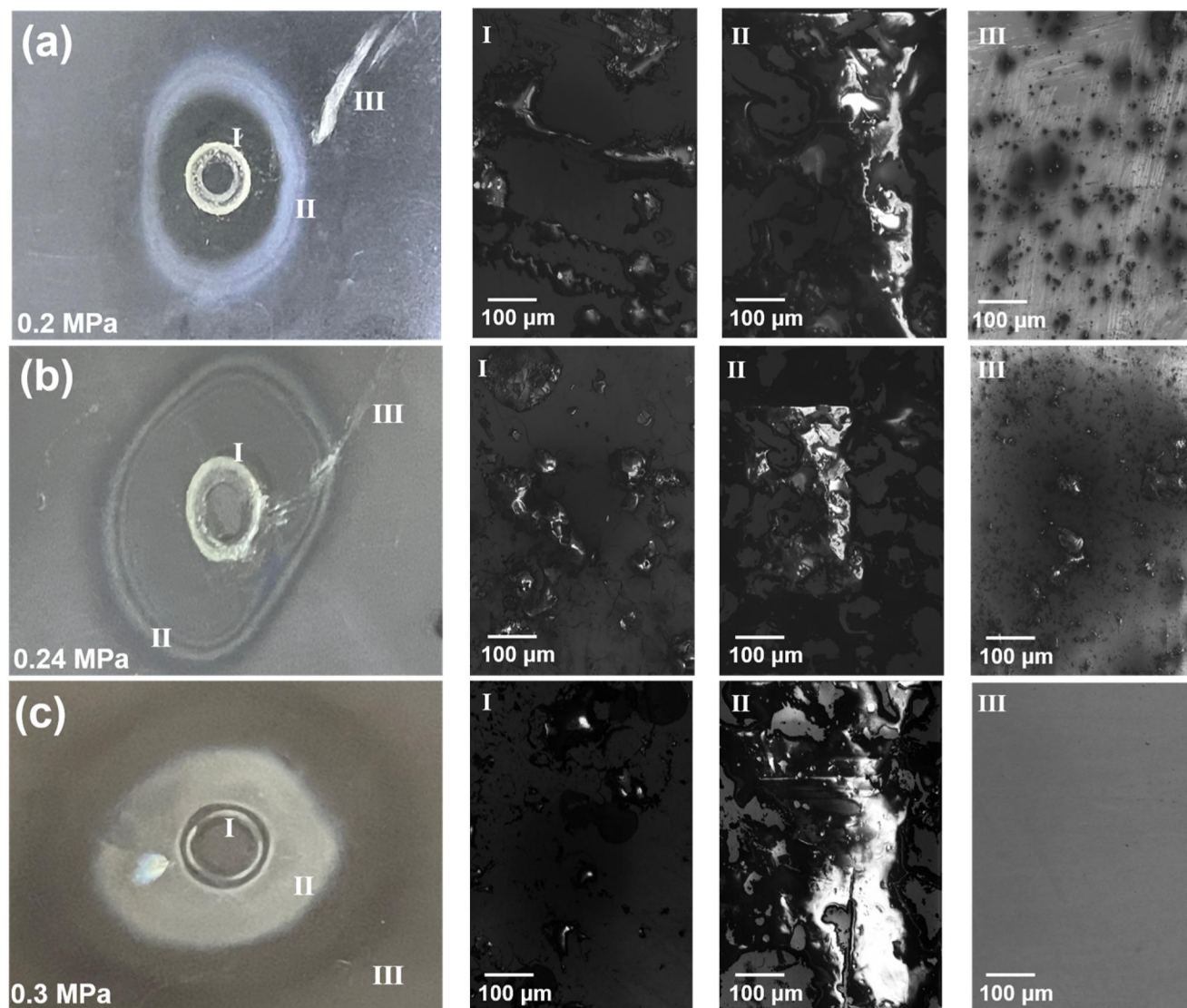


FIGURE 4 The surface morphology of the PET film changed after discharge under different gas pressure conditions. (a) 0.2 MPa. (b) 0.24 MPa. (c) 0.3 MPa.

F and N came from the decomposition products of C_4F_7N . Region II and III only have F and N elements. Among them, the F element in Region I and Region III is concentrated in the trace of morphological deterioration, indicating that the chemical reaction occurs in the flaky convex region and fluoride deposition occurs. In addition, the distribution intensity of F element in Region I is significantly higher than that of C element. The distribution intensity of C element in Region II is significantly higher than that of F and N, indicating that the morphological changes in this region are mainly due to the physical changes of PET electrical and thermal stress.

Figure 6 shows the statistical results of element content in different regions. It can be seen that the content of F and N elements in Region II is significantly lower than that the other two regions. There is only 1.6% F element and no N element is detected at 0.3 MPa, which indicates that Region II is basically

not involved in C_4F_7N -PET decomposition. The content of F and N elements in Region III were also lower than those in Region I. The content of F and N elements in Region I were 52.31% and 9.27% under 0.2 MPa, which were higher than that of 19.52% and 4.81% in Region III. The content of F and N in Region I were 38.21% and 8.25% at 0.24 MPa, which were much higher than that of 8.71% and 2.17% in Region III. Therefore, the chemical reaction intensity of the interaction between electrode and PET film interface is higher, which is also consistent with the more solid precipitates observed in Region I.

Figure 6d–f show the element content of Region I–III under different test conditions. The contents of F and N in the three groups of test conditions in Region I were 52.31%, 42.59% and 38.21% and 9.27%, 8.58% and 8.25%, respectively. The contents of F and N in Region II were 13.54%, 4.72% and 1.6% and 4.69%, 1.31% and 0%, respectively. The content of F

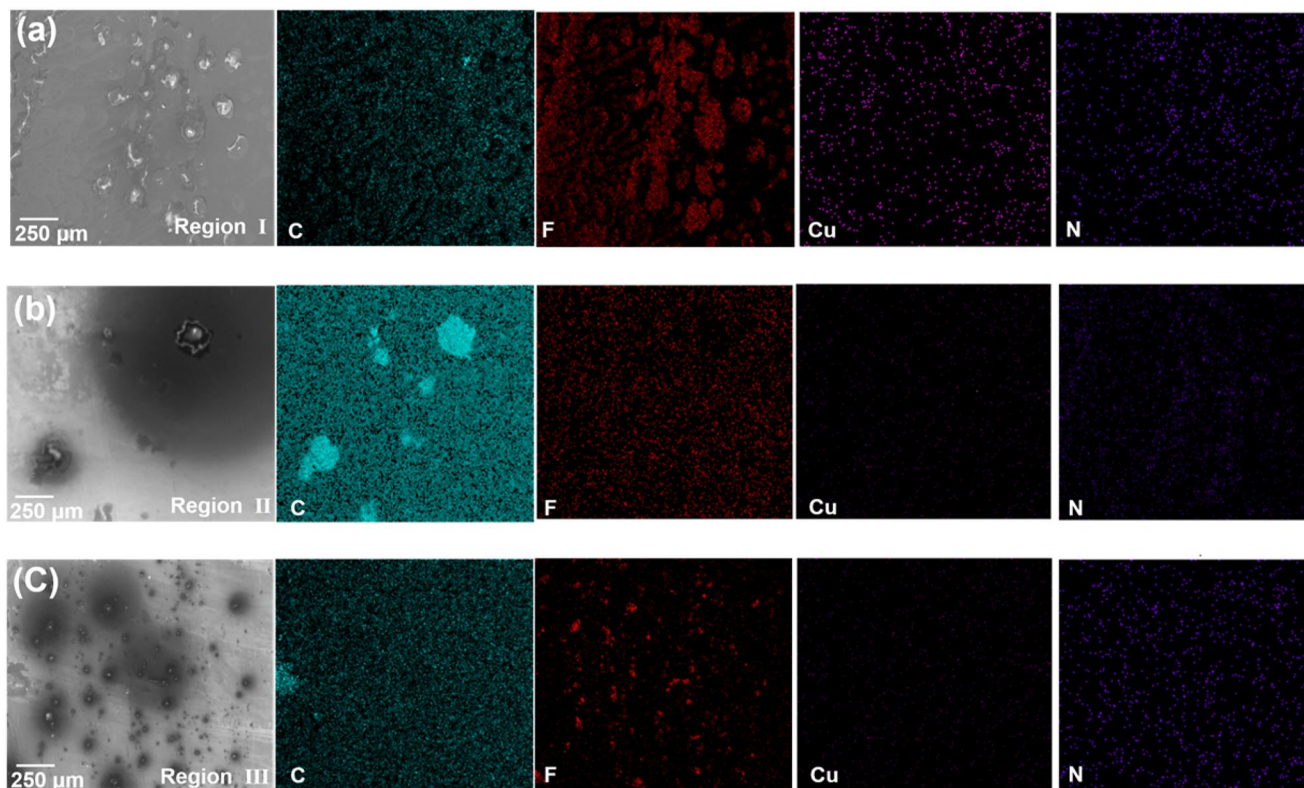


FIGURE 5 The distribution characteristics of elements in the three degradation regions of the PET film after discharge under 0.24 MPa. (a) Region I. (b) Region II. (c) Region III.

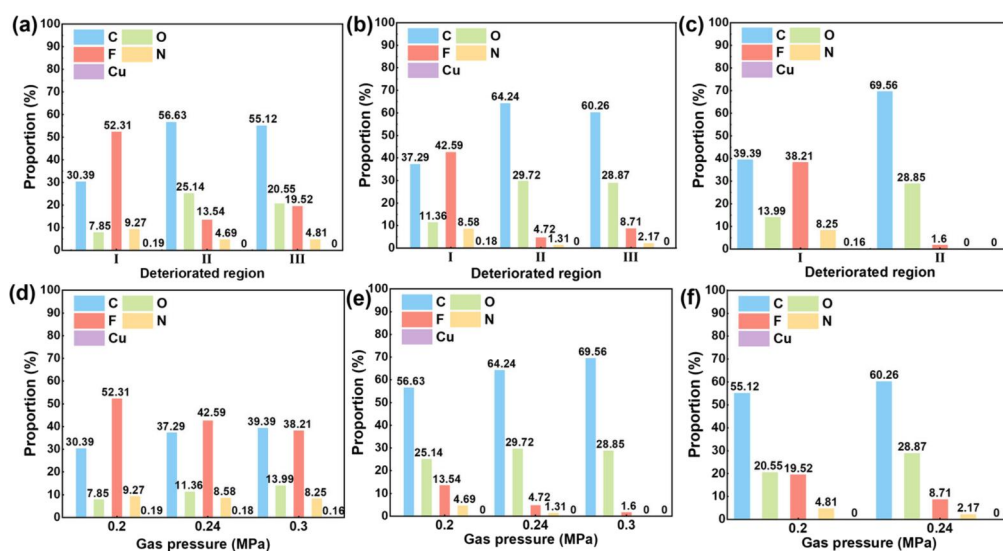


FIGURE 6 The comparison of element content after interface discharge of polyethylene terephthalate film. (a) 0.2 MPa. (b) 0.24 MPa. (c) 0.3 MPa. (d) Region I. (e) Region II. (f) Region III.

in Region III was 19.52% and 8.71% at 0.2 and 0.24 MPa, respectively, and the content of N was 4.81% and 2.17%, respectively. Therefore, with the increase of gas pressure, the content of F and N elements in the corresponding region showed a decreasing trend, which was consistent with the test results of gas decomposition products under different test conditions.

3.3 | The reaction mechanism between C_4F_7N and PET film

Combined with the decomposition characteristics of C_4F_7N , morphology change and element distribution characteristics of PET obtained above, we further analysed the reaction mechanism of gas–solid interface discharge induced decomposition.

The direct contact between the electrode and the PET film (Region I) has the highest electric field intensity, and the gas and gas–solid interface reactions are the most intense. On the one hand, C_4F_7N will be ionised to produce a series of positive and negative ions and free radicals. On the other hand, the PET film will react with various particles produced by C_4F_7N decomposition and produce solid precipitates. The similar process also occurs in the extended region (Region III) of interface discharge, while the energy generated in this region is less than Region I. Thus, the intensity of various physical and chemical reactions is lower and the amount of solid precipitates is less. In addition, the morphology change of the halo region (Region II) is due to the physical change of the PET film structure induced by electrical and thermal stress. At the same time, there is a possibility of reaction with the PET film in the intermediate product of C_4F_7N decomposition, which is manifested by the deposition of a small amount of F and N elements.

For gas decomposition products (CF_4 , C_2F_6 , C_3F_8 and C_2N_2), it is mainly composed of intermediate products produced by C_4F_7N dissociation. The main path and enthalpy of C_4F_7N decomposition reaction are given in Figure 7a. The enthalpy of path 1 is the lowest (74.94 kcal/mol), and it is more likely to occur. Figure 7b further gives the path and enthalpy value of the steady-state gas products produced by the

intermediate products. The energy released by the formation of small molecular products such as C_2N_2 and CF_4 is significantly higher than that of C_2F_6 and C_3F_8 , which is consistent with the fact that the content of CF_4 in the gas decomposition products is higher than that of C_2F_6 and C_3F_8 .

For solid precipitates, on the one hand, electrical and thermal stress will lead to the breakage of PET molecular chemical bonds, which will destroy the original structure of the film. On the other hand, the particles produced by the gas phase decomposition of C_4F_7N will also be deposited on the surface of the PET film. In addition, the intermediate products of C_4F_7N decomposition may react with PET at the gas–solid interface, resulting in the precipitation of solid products. Figure 7c shows the relaxation structure after the interaction between C_4F_7N decomposition particles and PET molecules. It can be seen that the generation of various complex structures releases energy, that is, the gas phase decomposition particles are coupled with PET to produce macromolecular substances and precipitate.

Moreover, the development process of interface discharge between gas mixture and the PET film were shown in Figure 8. The electric field intensity at the junction of the electrode and the PET film is relatively concentrated, so that the gas molecules nearby are first ionised to produce electrons

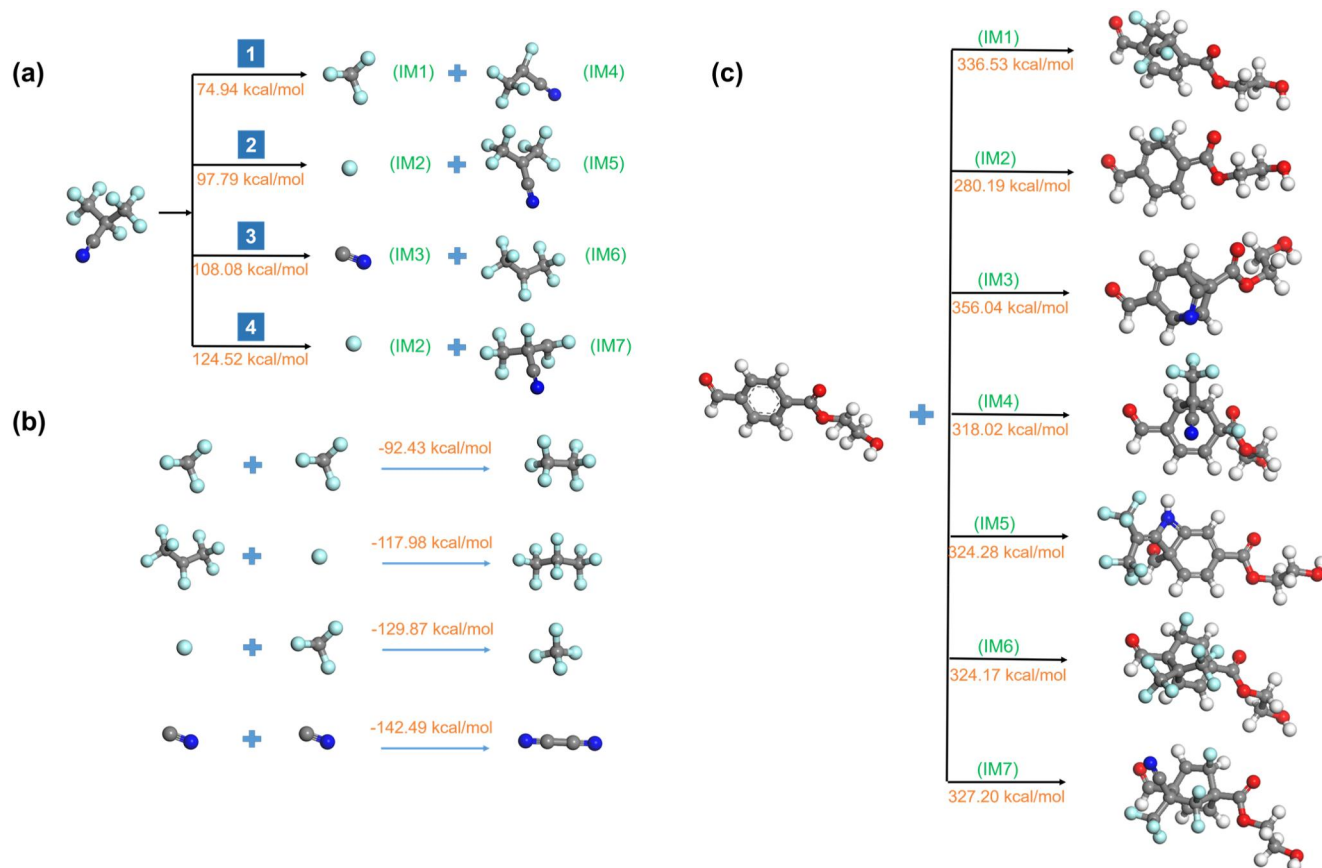


FIGURE 7 The reaction mechanism of interface discharge between C_4F_7N/CO_2 and the PET film. (a) The relevant decomposition mechanism of C_4F_7N . (b) The generation mechanism of gas by-products. (c) Possible reactions on the PET film.

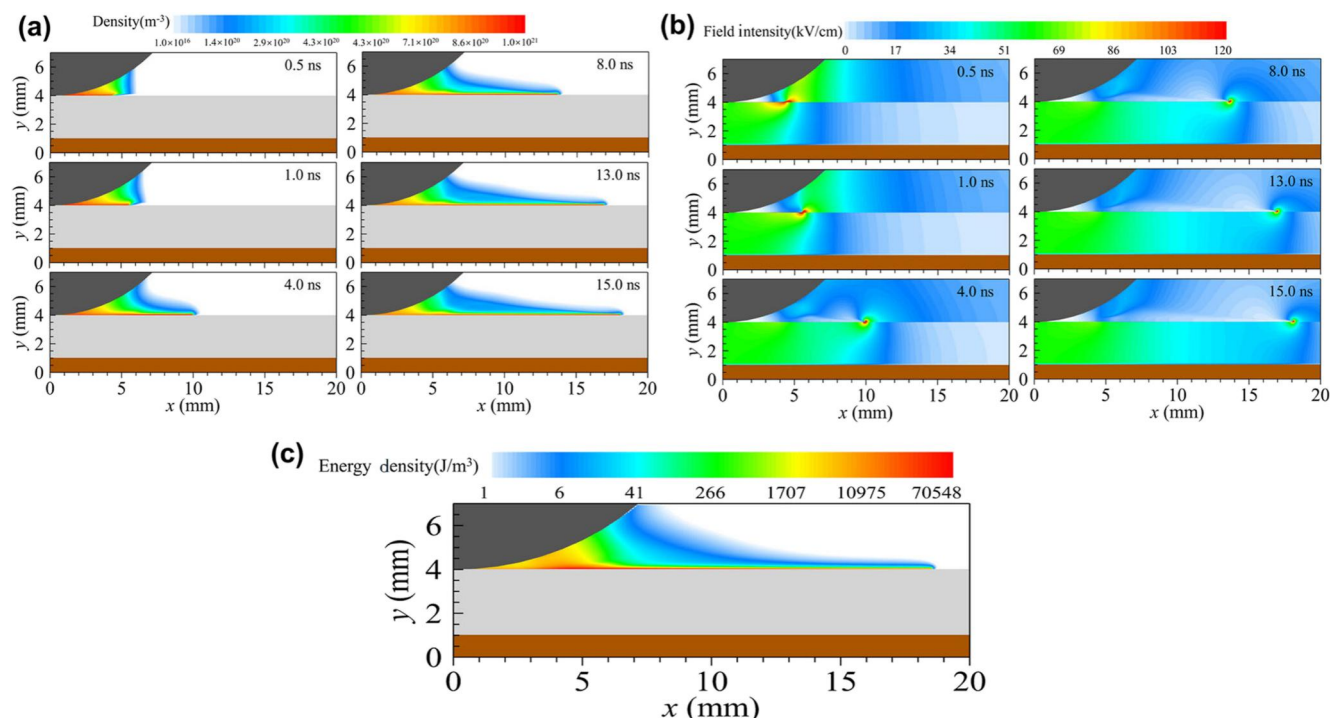


FIGURE 8 The variation process of interface discharge between C_4F_7N/CO_2 and the PET film. (a) The distribution of electron density. (b) The distribution of electric field. (c) Total energy density on the PET film.

(Figure 8a). Then the produced electrons collide with gas and solid molecules under the acceleration of electric field, which further induces ionization and promotes the generation of more electrons. These electrons are pushed away from the high voltage electrode and develop outward under the action of electric field with the variation of time. As the electrons are away from the high voltage electrode, the electron density distribution tends to be sparse. In the process of interface discharge, the varying regularity of electric potential distribution is shown in Figure 8b. It can be observed that the distortion degree of the front electric field becomes weaker with the increase of time, which also leads to the gradual weakening of the collision ionisation on the gas-film interface in the process of outward development until it disappears. Figure 8c gives the total energy density on the gas-film interface. During the development of interface discharge, most of the energy is concentrated near the electrode, and the energy density decreases gradually along the direction away from the electrode.

In our test, Region I directly contact with the electrode, and the energy density is the largest which results in the most intense reactions on the gas-PET film interface. It can be seen from Figure 8c that the energy of Region III (outward development trace) is less than that of Region I, so the intensity of various reactions is lower and the interface damage is also minor. The morphological change of the Region II (halo region) is mainly due to the physical change of the PET film structure caused by electrical and thermal stress, and the extent of damage is the lightest. Therefore, our test results show the consistency with the numerical simulation.

3.4 | Interface partial discharge characteristics of SF_6 and PET film

We further tested the interface discharge characteristics of SF_6 and PET. Figure 9 shows the morphology, elemental composition and gas product formation of PET after the test. The change of PET morphology is similar to that of C_4F_7N/CO_2 gas mixture and there is obvious deterioration after the test. Different from C_4F_7N/CO_2 gas mixture under 0.24 MPa, only Region I and II appear after SF_6 -PET interface discharge under this condition, and no external development trace (Region III) is generated, indicating that the interaction between SF_6 and PET is lower than that of C_4F_7N/CO_2 under the same pressure and applied voltage. The element distribution characteristics of the degradation region are similar to those of the C_4F_7N/CO_2 test, as shown in Figure 9b. Among them, Cu, F and S elements appear in Region I, and F element is concentrated in the degradation trace, while C element is concentrated in Region II. The significantly concentrated distribution of F element in the deterioration trace of Region I indicates that the reaction between the film and SF_6 in this region is more intense. This conclusion is also demonstrated by the comparison of element content in Figure 9c. Specifically, the contents of F and S elements in Region I are 15.87% and 1.96%, respectively, which are much higher than 4.75% and 0.65%, respectively, in Region II. Figure 9d shows the types and concentration changes of gas products after interface discharge of SF_6 and PET film. It can be seen that the content of CO_2 , CF_4 , SO_2 , SO_2F_2 , SOF_2 , and SOF_4 increases linearly with the discharge time. The presence of C element-containing gas

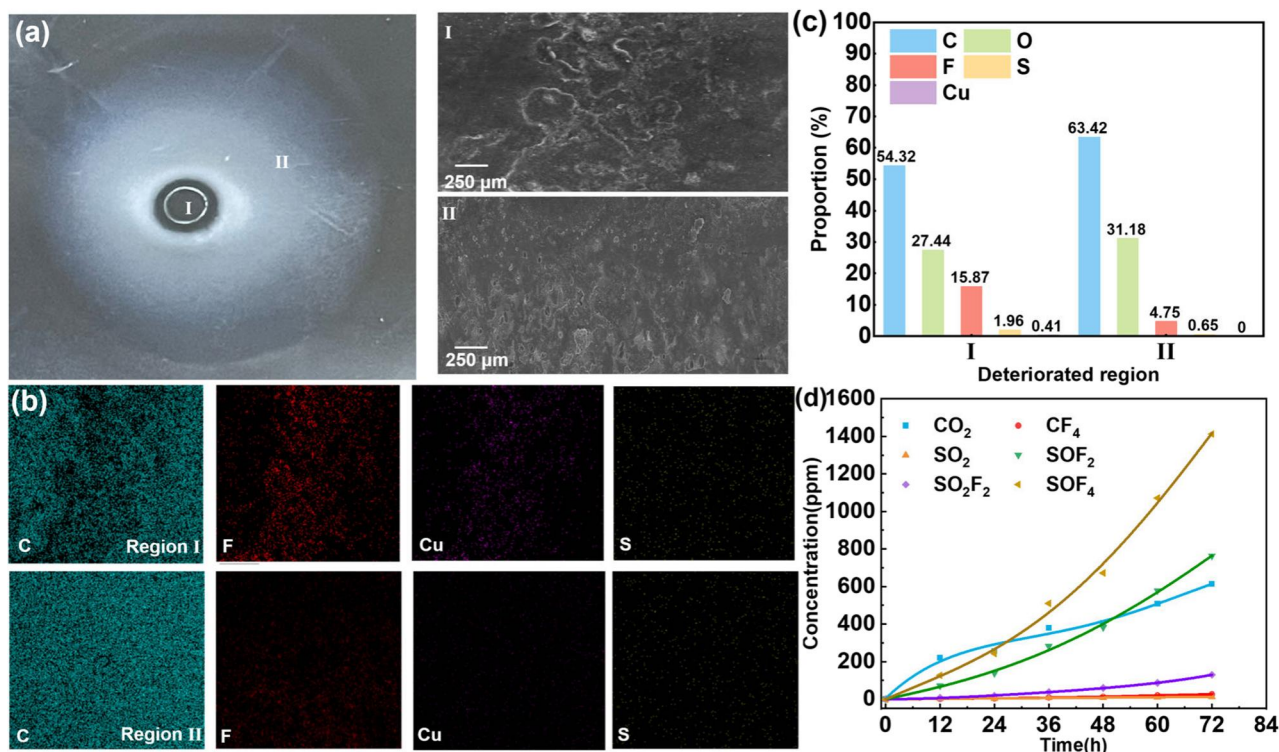


FIGURE 9 The interface discharge test of SF₆ and the PET film under 0.24 MPa. (a) Morphology change of polyethylene terephthalate film. (b) Distribution characteristics of elements in the degraded region of PET film. (c) Element content change of the PET film. (d) Interface discharge induced gaseous decomposition by-products of SF₆ and the PET film.

components confirmed that PET participated in the reaction process with SF₆ decomposition particles.

4 | CONCLUSION

In this paper, we investigated the interface PD decomposition characteristics of C₄F₇N/CO₂ gas mixture and the PET film for GIT. The characteristics of gas decomposition and solid morphology degradation under different pressure and mixing ratio were explored and compared with SF₆. Furthermore, the gas–solid interface reaction mechanism of C₄F₇N–PET was analysed. The following conclusions can be obtained:

- (1) The interface discharge of C₄F₇N/CO₂ and PET mainly produces four gas products: CF₄, C₂F₆, C₃F₈ and C₂N₂, among which the content of CF₄ is the highest. With the increase of gas pressure, the content of decomposition products decreases significantly, that is, the decomposition reaction of gas–solid interface is inhibited at high gas pressure. In engineering applications, it can be considered to increase the gas pressure appropriately to avoid the gas–solid interface decomposition.
- (2) Three degradation regions were generated at the PET after interface PD. Obvious gas–solid interface reactions occurred in the contact area with the electrode and the epitaxial development trace of interface discharge. The F

and N elements are also deposited in the deterioration region. The content of C element in the contact area with the electrode is significantly reduced and the content of F element is obviously increased. The content of F and N elements in the halo area is the lowest, and its deterioration is mainly caused by physical changes such as electrical and thermal stress.

- (3) Under the interface discharge of C₄F₇N–PET, there is a gas-phase and gas–solid interface interaction process. The particles generated by the decomposition of C₄F₇N and the relaxation of PET molecules will form a series of complex structural products, resulting in the precipitation of solid products. Under the same conditions, SF₆–PET interface discharge can also induce the change of film surface morphology, but the degree of deterioration is weaker than that of C₄F₇N/CO₂.

ACKNOWLEDGEMENTS

This work was funded by the National Natural Science Foundation of China (Grant Number: 51977159) and the fellowship of China Postdoctoral Science Foundation (Grant Number: 2022M712446).

CONFLICT OF INTEREST STATEMENT

The authors declare that there is no conflict of interest that could be perceived as prejudicing the impartiality of the research reported.

DATA AVAILABILITY STATEMENT

The data used to support the findings of this study is included within this paper.

ORCID

Song Xiao  <https://orcid.org/0000-0002-4749-4058>

Yifan Wang  <https://orcid.org/0009-0006-0633-0125>

Haoran Xia  <https://orcid.org/0009-0005-7153-3634>

Xiaoxing Zhang  <https://orcid.org/0000-0001-5872-2039>

Yi Li  <https://orcid.org/0000-0003-2236-895X>

REFERENCES

- Eteiba, M., Aziz, M.M.A., Shazly, J.H.: Sensitivity of steady-state temperatures of SF₆ gas-cooled-insulated power transformers to selected parameters. *IEEE T. Power Deliver.* 24(3), 1249–1256 (2009)
- Ozgonenel, O., et al.: Electrostatic analysis of SF₆ gas insulated distribution transformer. In: *National Conference on Electrical, Electronics and Biomedical Engineering (ELECO)*, pp. 359–362 (2016)
- Kudo, A., et al.: Development of 275 kV gas cooled type gas-insulated power transformer. *IEEE T. Power Deliver.* 8(1), 264–270 (1993)
- Tsukao, S., et al.: Application of gas insulated transformers to underground substations in Japan. In: *1st International Conference and Exhibition on Transmission and Distribution in the Asia Pacific Region*, pp. 517–521 (2002)
- Li, X., Zhao, H., Murphy, A.B.: SF₆-alternative gases for application in gas-insulated switchgear. *J. Phys. D Appl. Phys.* 51(15), 153001 (2018)
- Tian, S., et al.: Adsorption properties of environmentally friendly insulating medium C₄F₇N and its common decomposition products in NaA, NaZSM-5, and NaX molecular sieves. *High Volt.* 8(3), 611–621 (2023)
- Zhang, B., et al.: Ab initio molecular dynamics calculations on electron ionization induced fragmentations of C₄F₇N and C₅F₁₀O for understanding their decompositions under discharge conditions. *Phys. Chem. Chem. Phys.* 25(10), 7540–7549 (2023)
- Ai, X., et al.: The effect of electrode surface roughness on the breakdown characteristics of C₃F₇CN/CO₂ gas mixtures. *Int. J. Elec. Power* 118, 105751 (2020)
- Zhang, B., et al.: Arc interruption performance of C₄F₇N-CO₂ mixture in a 126 kV disconnector. *IEEE T. Power Deliver.* 38(2), 1197–1207 (2022)
- Xiao, S., et al.: Research on the adsorption of environmentally friendly insulating gas C₄F₇N decomposed components on the surface of γ-Al₂O₃. *High Volt.* 8(2), 274–282 (2023)
- Xiao, S., et al.: Insulation performance and electrical field sensitivity properties of HFO-1336mzz(E)/CO₂: a new eco-friendly gas insulating medium. *IEEE Trans. Dielectr. Electr. Insul.* 28(6), 1938–1948 (2021)
- Li, Y., et al.: Eco-friendly gas insulating medium for next-generation SF₆-free equipment. *iEnergy* 2(1), 14–42 (2023)
- Tu, Y., et al.: Feasibility of C₃F₇CN/CO₂ gas mixtures in high-voltage DC GIL: a review on recent advances. *High Volt.* 5(4), 377–386 (2020)
- Chen, G., et al.: Intrinsic hetero-polar surface charge phenomenon in environmental-friendly C₃F₇CN/CO₂ gas mixture. *J. Phys. D Appl. Phys.* 53(3), 708–714 (2017)
- Zheng, Y., et al.: Influence of conductor surface roughness on insulation performance of C₄F₇N/CO₂ mixed gas. *IEEE Trans. Dielectr. Electr. Insul.* 26(3), 922–929 (2019)
- Ye, F., et al.: Arc decomposition behavior of C₄F₇N/Air gas mixture and biosafety evaluation of its by-products. *High Volt.* 7(5), 856–865 (2022)
- Zhang, T., et al.: Insulation properties of C₄F₇N/CO₂ mixtures under lightning impulse. *IEEE Trans. Dielectr. Electr. Insul.* 27(1), 181–188 (2020)
- Tu, Y., et al.: Insulation characteristics of fluoronitriles/CO₂ gas mixture under DC electric field. *IEEE Trans. Dielectr. Electr. Insul.* 25(4), 1324–1331 (2018)
- Yang, Y., et al.: Influence of micro-water on AC breakdown characteristics of C₄F₇N/CO₂ gas mixture under non-uniform electric field. *High Volt.* 7(6), 1059–1068 (2022)
- Wu, S., et al.: Charge accumulation characteristics of SF₆-epoxy interface under negative repetitive nanosecond pulses. *CSEE J. Power Energ.* (2023)
- Qiu, Y., Kuffel, E.: Comparison of SF₆/N₂ and SF₆/CO₂ gas mixtures as alternatives to SF₆ gas. *IEEE Trans. Dielectr. Electr. Insul.* 6(6), 892–895 (1999)
- Wu, S., et al.: Towards the surface flashover in DC GIL/GIS: the electric field distribution and the surface charge accumulation. *Phys. Scripta* 97(7), 072001 (2022)
- Chen, G., et al.: Standardizing conductor surface roughness for DC gas-insulated equipment—a careful analysis on local morphology. *J. Phys. D Appl. Phys.* 55(23), 23LT01 (2022)
- Okabe, S., et al.: Partial discharge-induced degradation characteristics of insulating materials of gas-filled power transformers. *IEEE Trans. Dielectr. Electr. Insul.* 17(6), 1715–1723 (2010)
- Okabe, S., et al.: Study on decomposition gas for diagnostics of gas-insulated transformers. *Electr. Eng. Jpn.* 130(1), 48–58 (2000)
- Gao, Q., et al.: Negative corona discharge mechanism in C₄F₇N-CO₂ and C₄F₇N-N₂ mixtures. *AIP Adv.* 12(9), 095101 (2022)
- Zhang, B., et al.: Decomposition characteristics of C₄F₇N/CO₂ mixture under AC discharge breakdown. *AIP Adv.* 9(11), 115212 (2019)
- Fu, Y., et al.: Theoretical study on decomposition pathways and reaction rate constants of C₄F₇N with O atom. *J. Phys. D Appl. Phys.* 53(10), 105202 (2019)
- Wang, C., et al.: Decomposition characteristics and marker products of C₃F₇CN/EP insulation system with long-term surface discharge. *Eng. Fail. Anal.* 116, 104719 (2020)
- Yuan, R., et al.: Study of compatibility between epoxy resin and C₄F₇N/CO₂ based on thermal ageing. *IEEE Access* 8, 119544–119553 (2020)
- Holman, T.: *Gas Insulated Transformers (GYTs)*, pp. 8. University of Technology Sydney (2013)
- Zhang, X., et al.: Experimental study on power frequency breakdown characteristics of C₄F₇N/CO₂ gas mixture under quasi-homogeneous electric field. *IEEE Access* 7, 19100–19108 (2019)
- Kozuch, S., Martin, J.M.L.: Spin-component-scaled double hybrids: an extensive search for the best fifth-rung functionals blending DFT and perturbation theory. *J. Comput. Chem.* 34(27), 2327–2344 (2013)
- Islam, M.M., Strachan, A.: Decomposition and reaction of polyvinyl nitrate under shock and thermal loading: a ReaxFF reactive molecular dynamics study. *J. Phys. Chem. C* 121(40), 22452–22464 (2017)
- Yuan, C., et al.: Modeling interfacial interaction between gas molecules and semiconductor metal oxides: a new view angle on gas sensing. *Adv. Sci.* 9(33), 2203594 (2022)
- Zhang, R., et al.: Photogenerated carrier behavior at a gas–solid interface for CO₂ adsorption on Cs₂AgBiBr₆ nanocrystals. *Dalton T* 51(47), 17938–17941 (2022)
- Wang, C., et al.: Decomposition products and formation path of C₃F₇CN/CO₂ mixture with suspended discharge. *IEEE Trans. Dielectr. Electr. Insul.* 26(6), 1949–1955 (2019)
- Delley, B.: An all-electron numerical method for solving the local density functional for polyatomic molecules. *J. Chem. Phys.* 92(1), 508–517 (1990)
- Perdew, J.P., Burke, K., Ernzerhof, M.: Generalized gradient approximation made simple. *Phys. Rev. Lett.* 77(18), 3865–3868 (1996)
- Zhu, Y., et al.: Nanosecond surface dielectric barrier discharge in atmospheric pressure air: I. measurements and 2D modeling of morphology, propagation and hydrodynamic perturbations. *Plasma Sources Sci. Technol.* 26(12), 125004 (2017)
- Zhang, C., et al.: Evolution characteristics of DC breakdown for biaxially oriented polypropylene films. *IEEE Trans. Dielectr. Electr. Insul.* 30(3), 1188–1196 (2023)

How to cite this article: Xiao, S., et al.: Assessment on gas-polyethylene terephthalate solid interface partial discharge properties of C₄F₇N/CO₂ gas mixture for eco-friendly gas insulating transformer. *High Voltage.* 9(1), 35–45 (2024). <https://doi.org/10.1049/hve2.12421>